J. CHEM. SOC. FARADAY TRANS., 1992, 88(23), 3451–3459

Two β-Forms and the α-Helix of *N*-Octanoyl-L-glutamic Acid Oligomers

Toshiyuki Uehara, Hirofumi Okabayashi,* Keijiro Taga and Tadayoshi Yoshida
Department of Applied Chemistry, Nagoya Institute of Technology, Gokiso-cho, Showa-ku, Nagoya 466, Japan
Hiroshi Kojima
Gifu National College of Technology, Shinsei-cho, Motosu-gun, Gifu, 501-04, Japan

N-Octanoyl-L-glutamic acid oligomers (residue number, $N = 3$–6, 8, 10, 12, 14, 16, 18, 20 and 22) have been synthesized in order to study their molecular conformations in the solid state. The X-ray diffraction powder patterns and the vibrational spectra of these oligomers have been investigated and compared with those of two β-forms (β_1 and β_2) and the α-helix of poly(L-glutamic acid).

The results are summarized as follows. These oligomers take up a β_1- or β_2-like structure, similar to that of the two β-forms of poly(L-glutamic acid). The methods used to precipitate the samples are related to the conformational preferences in the solid state. $\beta_1 \leftrightarrow \beta_2$ interconversion is possible by reprecipitation of the sample. Preferential stabilization of the β_1- or β_2-forms is strongly dependent on the residue number. Films of the oligomers, made by casting them from a dimethylformamide solution onto NaCl or KBr plates, take up an α-helical structure, and the $\alpha \rightarrow \beta_1$ or $\alpha \rightarrow \beta_2$ transition depends on the residue number of the cast film.

Recently, it has been shown that a bacterial photosynthetic reaction-centre protein could be crystallized in the form of protein–surfactant complexes in the presence of surfactant molecules,[1–3] and the structure of the surfactant–protein assembly has been determined.[4] It has also been shown that surfactant molecules promote the ordered packing of protein–surfactant complexes.[5,6] This ordered packing may then change the conformation of the protein molecule in a protein–surfactant complex. Much attention is being given to the mechanism of the conformational change promoted by the ordered packing. However, the membrane protein–surfactant complex is a so-called 'giant assembly'. Therefore, for a detailed study of such conformational changes, further studies of model systems may also be required.

In fact, association often brings about the conformational change of a molecule, thus producing an assembly. For example, in cases of simple saturated and unsaturated surfactants, conformational preference accompanies micellization.[7–10] This process may also apply in the case of a giant assembly.

Our attention has been focused on the conformational change of a surfactant molecule containing oligopeptides. We have previously reported that the polyglycine II (PGII)-like helical structures in *N*-acylglycine oligomers ($N = 3$–5) are promoted by long acyl chains.[11] For the *N*-acyl glycine oligomers, the long hydrocarbon chains seem to cause an ordered packing state of the oligomers and to induce a further PGII-like structure in the NH···O=C and peptide skeletons. However, with the exception of these glycine oligomers, very little is known about the long-acyl-chain effect on the conformations of oligopeptides in the ordered packing state. Furthermore, it has been shown that preferential stabilization of the helical structure for the anions of *N*-acylglycine oligomers is promoted by intermolecular association of the anions in aqueous solution and the helical structure is also stable in the hydrophobic environment of micelles.[12] Probably, for *N*-acyl derivatives of oligopeptides, the long-acyl-chain effect and the conformational preference on micellization strongly depend upon the amino acid residue. It is therefore desirable to conduct further studies on *N*-acyl homo-oligopeptides having the various kinds of amino acid residues or *N*-acyl hetero-oligopeptides. The results of such studies will provide basic and important contributions to the understanding of the structure of membrane proteins, which at present remains largely unresolved.

Many studies of small oligopeptides have already been carried out and the influence of the degree of polymerization (DP) on their conformations has been discussed.[13–19] The circular dichroism (CD) behaviour of the L-glutamic acid oligomers [CH_3CO—$(Glu)_n$—$NHCH_2CH_3$] having DP values of 1–50 has been compared with that obtained with the polymer, and their CD spectra in aqueous solution have been interpreted in terms of a combination of the four possible conformations: α-helix, β-sheet, random and extended structures.[18] Furthermore, by using CD, the existence of a critical range of DP values (8–10) for β-structure formation has also been clearly demonstrated in solution, and, using optical rotatory dispersion, the formation and stability of β-structures in solution have also been measured as a function of temperature and concentration.[19]

For the polyoxyethylene (POE)-bound α-L-glutamic acid oligomers, residue number $N \leqslant 20$,[20] it has been concluded that the formation of an α-helical structure starts at $N = 7$ and that the conformational behaviour of the POE-bound and free peptides is identical. However, when the long acyl groups, rather than POE, are bound to α-L-glutamic acid oligomers, we may assume that the long-acyl-chain effect causes the critical size of the α-helix appearance to change.

α-Helical- and β-structures of poly(L-glutamic acid)[poly(Glu)] or its alkaline-earth-metal salts in the solid state and aqueous solution have been investigated in detail by circular dicroism,[18,21–23] vibrational spectra,[21,23–32] X-ray diffraction[21,33–36] and other methods.[37–43]

Keith *et al.*[33,34] have found two modifications of β-poly(L-glutamic acid) and have proposed crystal structures from an analysis of X-ray powder patterns, which were based on Pauling and Corey's antiparallel-chain pleated-sheet model.[44] The results show that one of the two modifications provides the intersheet spacing of 8.8 Å and another modification gives rise to a smaller intersheet spacing (7.8 Å). They have also proposed that the thicknesses of the crystalline lamellae are in the range 25–60 Å in β-crystals and are *ca.* 100 Å in α-crystals. Moreover, the poly(Glu) molecule crystallizes by folding at the upper and lower surfaces of the crystals.

Itoh *et al.*[21] have found that a temperature-induced α-helix to β-sheet transition for α-poly(Glu) provides two β-forms (β_1

and β_2). Heating of poly(Glu) from 313 to 358 K brings about the β_1-form and temperature elevation above 358 K causes the $\beta_1 \rightarrow \beta_2$ transition. Conformational studies of the two β-forms have also been made by X-ray diffraction.[21] The structural differences between the two β-forms may be summarized as follows. The intersheet distance is 9.03 Å for β_1 and 7.83 Å for β_2, corresponding to the intersheet distances of 8.8 and 7.8 Å, respectively, for the two modifications found by Keith *et al.*[34] Therefore, the spacing found by Itoh *et al.*[21] is slightly different from that reported by Keith *et al.*[34] The pleated sheets of the β_2 form are more tightly packed, compared with those of the β_1 form. Itoh *et al.*[21] have also assumed that in the β_1 structure there are larger cavities between the neighbouring sheets, and water molecules within the cavities are hydrogen bonded to the peptide groups or to the carboxyl groups, thereby stabilizing the β_1 form.

However, detailed studies of the critical size for the appearance of the β_1–β_2, α–β_1 and α–β_2 conversions and for the appearance of the folding structure have not yet been made, in spite of their importance.

In this present study, we have synthesized a series of *N*-octanoyl-L-glutamic acid oligomers (oct-oligomers) in order to challenge both these problems and the long-acyl-chain effect mentioned above. Conformational studies of these oligomers have been made by analysing X-ray diffraction powder patterns and Raman and IR spectra.

In particular, vibrational bands characteristic of the secondary structures of poly(Glu) and evidence from X-ray powder patterns are important as references for interpretation of the vibrational spectra of the *N*-octanoyl-L-glutamic acid oligomers. Ambrose and Elliott[45] have found that the secondary structures of polypeptides are distinctly reflected in the amide A, I and II modes characteristic of the peptide groups (see footnote to Table 2, later). Furthermore, Miyazawa and Blout,[46] have elucidated that the secondary structure dependence of these vibrational modes arises from the vibrational interaction between the peptide groups. It has also been found that the amide V modes and the vibrational bands in the low-frequency region provide ample evidence for the existence of such secondary structures.[47] These vibrational modes have been successfully used to study the secondary structure of a great number of polypeptides and proteins. In this study, the vibrational modes characteristic of the α-helix and two β-forms of poly(Glu)[21,29,32] become a powerful tool in discussion of the conformations of the oct-oligomers.

Experimental

Materials

N-Octanoyl-L-glutamic acid oligopeptides were prepared by a stepwise procedure, as follows. *N-tert*-Butoxycarbonyl-L-glutamic acid α,γ-dibenzyl ester oligomers (BOC Glu oligomer dibenzyl esters) were prepared from *N-tert*-BOC-L-glutamic acid γ-benzyl ester and L-glutamic acid α,γ-dibenzyl ester toluene *p*-sulfonate in dichloromethane in the presence of triethylamine. The usual 1-ethyl-3-(3-dimethylaminopropyl)carbodiimide (EDC) method[48] was used for the condensation reaction. For the BOC Glu oligomer benzyl esters thus obtained, confirmation of the residue number (N) was made by proton NMR: the value of N was obtained from the relative peak areas of the ^{1}H resonance peaks arising from the BOC CH_3 groups and those of the benzyl protons. The BOC groups of these oligomers were removed by the action of hydrogen chloride in ethyl acetate. The BOC-free oligomer benzyl esters were coupled with the fatty acid in dichloromethane by the EDC method.[48] The coupling reaction was confirmed by thin-layer chromatography.

The *N*-octanoyl-L-glutamic acid oligomer benzyl esters were recrystallized in dichloromethane. Short oligomer benzyl esters (N = 3–8) were identified by elemental analysis. For the longer oligomers, the residue number was also confirmed by measurement of the relative proton NMR signal intensities of the *N*-octanoyl protons and the benzyl protons.

The α,γ-dibenzylesters of *N*-octanoyl-L-glutamic acid oligomers were recrystallized in dichloromethane–ethanol, and then, for these dibenzyl esters of the oligomers, debenzylation was performed in dimethylformamide (DMF) in the presence of Pd black. Debenzylation was confirmed by observing the disappearance of the vibrational bands arising from the benzyl groups.

The residue was then dissolved in DMF and dried diethyl ether was added to the solution until a precipitate appeared. The precipitate was then collected by filtration and dried (A-series samples).

The A-series samples were dissolved in DMF, and then the solvent was removed by evaporation in a vacuum system. The resulting solids were washed with dry acetone several times and dried (B-series samples). For the longer oligomers (N = 16–22) of the A-series, the samples were dissolved in saturated LiBr aqueous solution, and then distilled water was added. The resulting precipitate was collected by filtration and washed with dried acetone (C-series samples).

The residue numbers (N) of the *N*-octanoyl-L-glutamic acid oligomers (oct-oligomers) synthesized for the present study were 3, 4, 5, 6, 8, 10, 12, 14, 16, 18, 20 and 22.

Methods

Raman spectra below 4000 cm^{-1} were measured with a JEOL JRS-400D Raman spectrometer using 514.5 nm excitation. Infrared spectra were recorded on a Perkin-Elmer 1700 Fourier-transform infrared (FTIR) spectrometer (4000–400 cm^{-1}, with the sample dispersed in KBr discs and with films cast onto an NaCl plate) and on a JEOL FIR-100 FTIR spectrometer (400–50 cm^{-1}, with the sample dispersed in Nujol and sandwiched between two polyethylene windows).

X-Ray diffraction powder patterns were obtained by the use of an RAD-RC diffractometer with counter-monochromator (Cu-Kα, 60 kV, 200 mA).

Results and Discussion

X-Ray Diffraction Powder Patterns of Oct-oligomers and their Crystalline Modification

Uehara *et al.*[49] have previously measured and compared the X-ray diffraction powder patterns of the oct-oligomers with those of two β-forms (β_1 and β_2) or poly(Glu).[21] The results indicate that β_1- or β_2-type conformations are possible even in the oct-oligomers (N = 3–14) and the stability of the two β-forms in the solid state is dependent on the residue number.

In the present study, the X-ray diffraction powder patterns were measured for the A-, B- and C-series of the oct-oligomers, which also included the longer oligomers (N = 16–22) additionally synthesized for this work. The following results were obtained.

The samples of the shorter oligomers (N = 3–6) for the A-series provided β_2-type X-ray diffraction powder patterns, whereas the longer oligomers (N = 8–22) of the A-series gave β_1-type patterns. When the X-ray diffraction powder patterns were measured at room temperature for the A-series samples kept at −20 °C for six months, the β_2-type patterns of the shorter oligomers (N = 3–6) and the β_1-type patterns of the

longer oligomers (N = 16–22) remained unchanged, while the patterns for the medium length oligomers (N = 8–14) of the A-series had changed to those typical of β_2 type. Therefore, the β_2-type structure of the shorter oligomers and the β_1-type structure of the longer ones are very stable. However, the β_1-type structure of the medium length oligomers is less stable and is easily transformed to the β_2 type. The B-series samples (N = 3–22), which were precipitated directly from DMF, provided β_2-type powder patterns, which remained unchanged even after being kept at −20 °C for six months. Furthermore, the C-series samples (N = 16–22) provided β_2-type X-ray powder patterns, showing that the β_1-like structure of the longer A series (N = 16–22) can be converted to the β_2-like one by treatment in saturated LiBr–H_2O. These results imply that the method used to precipitate the sample affects the crystalline modification of the oligomer and that this modification further depends upon the residue number. The observed lattice spacings of the oct-oligomers characteristic of β_1- and β_2-type skeletal structures are summarized in Table 1.

Fig. 1 shows a schematic representation of two β-forms for the octamer of an oct-oligomer, which are based on the molecular models proposed by Keith *et al.*[34] In the β_1-type of oligomer, the carboxyl groups of the side chains belonging to different molecules may form hydrogen bonds with each other and produce cavities which may be filled by water molecules. In the β_2 type, the side chains probably interpenetrate more deeply, resulting in smaller intersheet spacing.

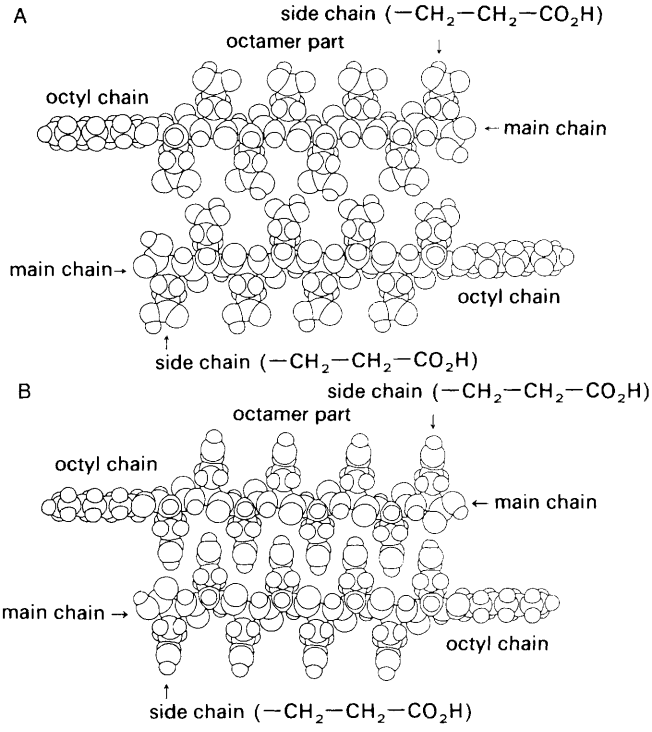

Fig. 1 Schematic representation of the two β-forms [β_1(A) and β_2(B)] for the octamer of oct-oligomers. In this schematic model, alignment and packing features of the octyl chains are not shown. A detailed study by X-ray powder patterns is now in progress and will be reported separately

Vibrational Spectra of the Oct-oligomers and the Two β-Forms

Fig. 2 shows the Raman spectra of the A- and C-series oligomers in the solid state. For the A-series, the spectral features of the shorter oligomers (N = 3–6) are quite different from those of the longer oligomers (N = 8–22). The Raman bands observed for the shorter oligomers are sharper than those of the longer ones, and their spectral features are very similar to those of the β_2-type poly(Glu).[21] The higher crystallinity or the higher-order degrees of the shorter oligomers may account for this observation, as has already been discussed in the case of the polymer.[21]

In the Raman spectra of the shorter oligomers, bands characteristic of the β_2-type poly(Glu) are observed (Fig. 2A), while for the longer oligomers Raman bands characteristics of the β_1-type polymer appear,[21] as seen in Fig. 2B and C. The Raman spectra of the C-series (Fig. 2D) are definitely characteristic of the β_2-type structure, although the characteristic bands of the unconverted β_1-types still remain. For the oct-oligomers, the Raman and IR band frequencies characteristic of the two β-types of poly(Glu) are summarized in Tables 2 and 3. For ease of discrimination between β_1- and β_2-like conformations in the oligomers, the vibrational bands characteristic of two β-forms of poly(Glu) are also listed in Tables 2 and 3 together with tentative assignments.[21,29,50,51]

For short oligomers, the observed frequencies of the amide I, II, III, IV and V modes and the skeletal vibrations are obviously characteristic of β_2-poly(Glu),[21] as seen in Table 3.

Fig. 3A shows the IR spectra of the β_2-type oligomers in the solid state in the low-frequency region, and the observed band frequencies are listed in Table 3. The IR bands at 232–239, 317–321, 443–448, 480–483 and 492–495 cm^{-1} are common to each short oligomer, and closely correspond to the bands at 240, 318, 450, 483 and 500 cm^{-1}, respectively,

Table 1 Observed lattice spacings (Å) of *N*-octanoyl-L-glutamic acid oligomers characteristic of β_1- and β_2-type structures[a]

β_2-type oligomers (N)[b]				β_1-type oligomers (N)[b]		
(3–6)	(8–14)	(16–22)	β_2-type poly(Glu)[c]	(8–14)	(16–22)	β_1-type poly(Glu)[c]
				9.00–9.32 w	9.02–9.04 m	9.03 s, d
7.66–7.84 m	7.87–7.93 m	7.89–7.97 m	7.83 w			
4.70–4.74 s	4.67–4.70 s	4.71–4.75 s	4.74 s	4.63–4.64 vs	4.60–4.62 vs	4.73 vs
3.91–3.96 vs	3.93–3.96 vs	3.90–3.95 vs	3.90 vs	3.89–3.93 s	3.79–3.89 m	3.89 s
3.57–3.62 m	3.58–3.63 m	3.61–3.69 s	3.61 s			
3.40–3.45 w	3.42–3.43 m	3.48–3.50 m	3.43 w			3.47 w
3.11–3.19 w	3.16–3.21 m	3.19–3.28 m	3.17 vs, d			
					2.63–2.97 vw	3.03 m
2.61–2.66 w	2.61–2.63 w	2.61–2.62 w	2.60 s	2.61–2.80 vw	2.77–2.86 vw	2.80 m
2.30–2.34 vw	2.30–2.32 vw	2.31–2.33 vw	2.31 w	2.26 vw	2.21–2.35 vw	2.22 w, d
1.95–2.00 vw	1.96–1.98 vw		1.98 w			

[a] s, strong; m, medium; w, weak; d, diffuse; v, very. [b] N = residue number. [c] Ref. 33, 34.

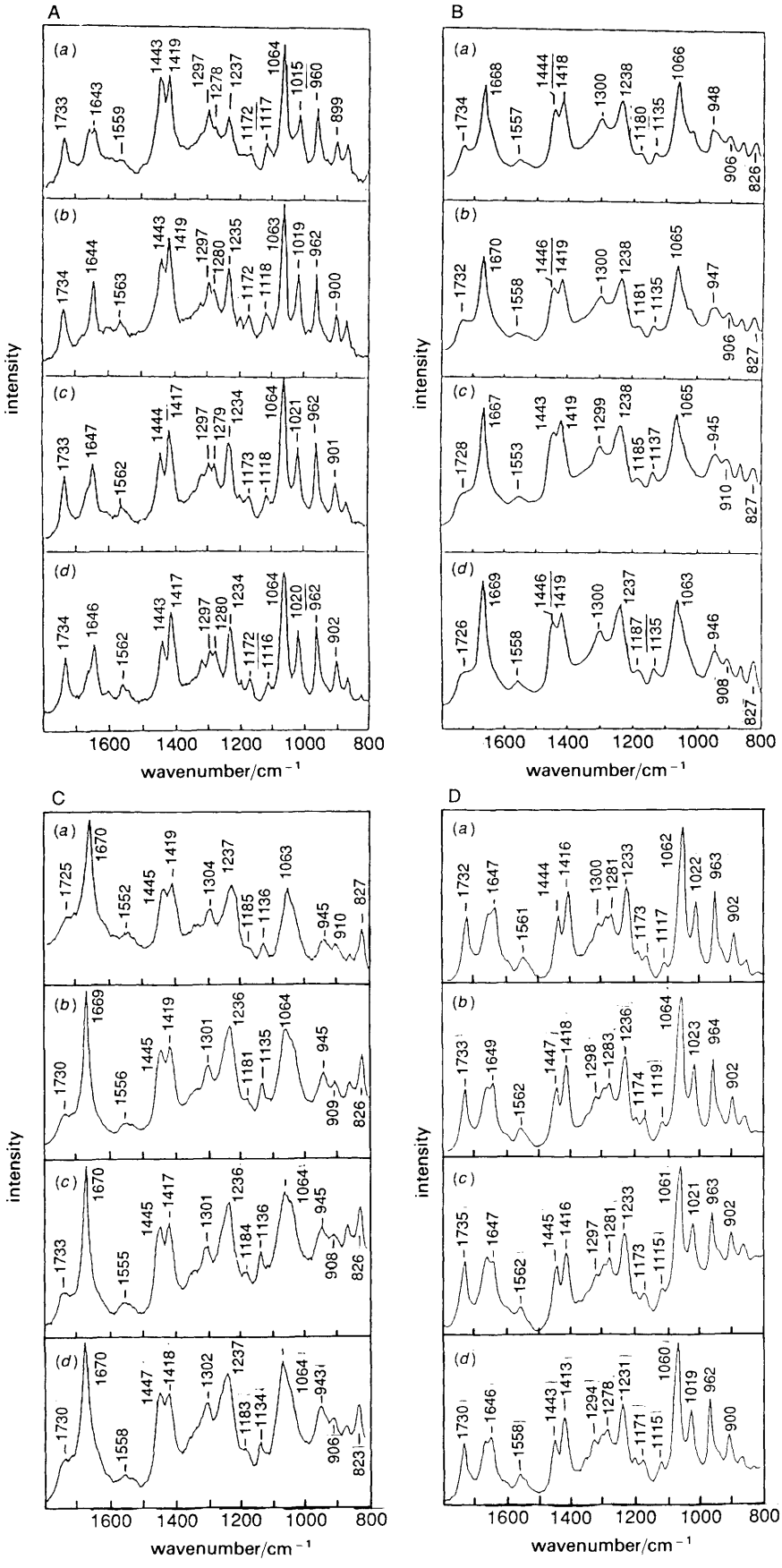

Fig. 2 Raman spectra of oct-oligomers: A, (A-series samples, $N = 3$–6, β_2-type), $N = 3$ (*a*), 4 (*b*), 5 (*c*), 6 (*d*); B, (A-series samples, $N = 8$–14, β_1-type), $N = 8$ (*a*), 10 (*b*), 12 (*c*), 14 (*d*); C, (A-series samples, $N = 16$–22, β_1-type), $N = 16$ (*a*), 18 (*b*), 20 (*c*), 22 (*d*); D, (C-series samples, $N = 16$–22, β_2-type), $N = 16$ (*a*), 18 (*b*), 20 (*c*), 22 (*d*). N is the residue number of the oligomer

Table 2 Observed vibrational band frequencies (cm^{-1})[a] characteristic of β_1-type oct-oligomers (A-series) in the solid state and tentative assignments

A-series (N)[b]						
(8–14)		(16–22)		β_1-type poly(Glu)[c]		
Raman	IR	Raman	IR	Raman	IR	assignm.[c,d]
3284–3286[e] w, br	3292[e] s	3281–3284[e] w, br	3291–3293[e] s			amide A
	(3297)[f]		(3309)[f]			
	3081–3084[e] m		3080–3082[e] m			amide B
1726–1734 vw	1714–1716 vs	1730–1733 vw	1713–1716 vw	1726 vw	1711 vs	ν[C=O(COOH)]
1667–1670 vs		1669–1670 vs		1672 vs		amide I
1652–1656 sh		1656 sh		1660 sh		
	1631–1638 vs		1630–1633 vs		1625 vs	
1553–1558 vw		1550–1556 vw		1556 vw		amide II
1537–1541 sh	1535–1541 s	1528–1540 vw	1529–1534 s	1535 sh	1523 s	
1443–1446 m	1444–1448 m	1445–1447 s	1447–1448 m	1444 m	1444 m	$s(CH_2)$
1418–1419 s	1409 1414 m	1417–1419 s	1410 m	1416 s	1414 m	
1336–1340 sh	1334–1339 w	1336–1340 w	1338–1340 w	1338 w	1336 w	def(CH) + $w(CH_2)$
1299–1300 m		1301–1304 m		1306 m		
1253–1257 sh	1257–1260 m	1253–1257 sh	1258–1259 m	1257 sh	1254 m	amide III
1237–1238 s	1218–1232 m	1236–1237 s	1229–1230 m	1236 s	1230 w	$w(CH_2)$
	1208–1218 sh		1216–1217 m		1208 w	
1180–1187 vw	1172–1181 m	1181–1185 vw	1176–1179 m	1186 w	1175 w	$t(CH_2)$
1135–1137 w	1133–1136 w	1134–1136 w	1134–1135 w	1137 w	1137 w	
1063–1066 s		1070–1074 sh		1072 m		ν(C—N, C—O)
1049–1052 sh		1063–1064 s		1062 m		
1039–1043 sh	1028–1039 vw	1041–1045 s	1029–1035 vw	1042 m		
1005–1009 sh		1005–1009 vw		1005 w		
945–948 m	945–951 vw	943–945 m	942–944 vw	944 m	952 vw	ν(C—O)
	932–939 vw		934–935 vw		932 w	
906–910 m		906–910 w		910 w		
826–827 w	819–825 vw	823–827 m	821–825 vw	825 m	822 w	$r(CH_2)$
	692–702 w	694–698 vw	698–702 w	705 vw	698 w	amide V
621–626 vw		636–647 vw		620 vw	630 vw	amide IV
573–579 vw		568–575 vw		576 vw		amide VI
		515–521 vw	529–530 vw		520 vw	δ[C=O(out)]
488–494 w	494–497 vw	486–496 vw	496–508 vw	492 vw		δ[C=O(in)]
	484–486 vw		485–489 vw			
	442–443 vw		440–447 sh			
398–403 vw	415–416 vw	399–406 vw	414–418 vw	403 vw	413 vw	backbone deformation
328–331 vw	333–335 vw	326–339 vw	330–334 w	328 vw		
274–281 vw		271–281 vw	305–307 vw	276 vw	298 w	
217–226 vw	244–246 w	219–226 vw	243–245 w	220 vw	230 w	
	149–150 vw		145–149 vw			

[a] s, strong; m, medium; w, weak; v, very; sh, shoulder; br, broad. [b] Only the main vibrational bands characteristic of β_1-type are listed. [c] From ref. 21 and 29. [d] ν, stretching; s, scissoring; t, twisting; w, wagging; r, rocking; δ, deformation; out, out-of-plane; in, in-plane; amide I, mainly C=O stretching vibration; amide II, N–H in-plane bending vibration coupled with amide C—N stretching; amide III, mainly amide C—N stretching vibration; amide IV, mainly skeletal deformation of peptide skeleton; amide V, mainly N—H out-of-plane bending vibration; amide VI, mainly out-of-plane deformation of peptide skeleton; amide A, N—H stretching and amide B, the overtone mode of amide II.[37,38] [e] Observed frequency. [f] Corrected for Fermi resonance using the equation of $\nu_{\text{amide A}}$(unperturbed) = $\nu_{\text{amide A}}$(perturbed) − [2($\nu_{\text{amide II}}$) − $\nu_{\text{amide B}}$(perturbed)]. The averaged values of the observed frequencies for amide A, amide B and amide II were used for calculation of these corrected frequencies.

for the β_2-type polymer.[21] The presence of these IR bands directly indicates that the short oligomers take up conformations similar to that of the β_2 form of poly(Glu).

For the long oligomers (N = 8–14 and 16–22 series), the vibrational spectral features are quite different from those of the short oligomers (Fig. 2B and 2C, and Tables 2 and 3), and on the whole, these vibrational spectra are characteristic of the β_1-type poly(Glu).[21] The amide I, II and III bands of the long oligomers correspond well to those of β_1-poly(Glu).[21] Moreover, the IR bands at 692–702 cm^{-1}, observed for all the long oligomers (N = 8–22), can be assigned to the amide V modes and provide direct evidence of the β_1-type structure.[21,52]

For these β_1-like oligomers, the IR bands at 243–246, 330–335, 484–489, 494–508 and 529–530 cm^{-1} are always seen (Fig. 3B). The two former bands (243–246 and 330–335 cm^{-1}) are much closer in frequency to the 240 and 318 cm^{-1} bands of the β_2-type polymer than they are to the 230 and 298 cm^{-1} bands of the β_1-type polymer.[21] Furthermore, the IR bands at 484–489 and 494–508 cm^{-1} correspond well to those at 483 and 500 cm^{-1} for the β_2-type poly(Glu), while those at 529–530 cm^{-1} can be compared with that at 520 cm^{-1} for the β_1-poly(Glu). On the whole, the IR spectral features of the β_1-like oligomers in the low-frequency region are very similar to those of the β_2-type poly(Glu). Thus, we may conclude that the β_1-like oligomers have conformations similar to that of the β_2-type poly(Glu) in the peptide skeleton. In fact, it has been suggested that the backbone structures of β_1- and β_2-poly(Glu) are similar to each other.[21] However, it may be noted that there is a more marked similarity of the peptide skeleton of the β_1-like oligomers to that of β_2-poly(Glu) than there is between the skeletal structures of the two β-forms of poly(Glu).

The $\beta_1 \rightarrow \beta_2$ transition for the A series samples could also be confirmed by observation of the IR bands in the low-frequency region. When the FTIR spectra of the β_1-type

Table 3 Observed vibrational band frequencies (cm^{-1})[a] characteristic of β_2-type oct-oligomers (B-series) in the solid state and tentative assignments

B-series (N)[b]						β_2-type poly(Glu)[c]		
(3–6)		(8–14)		(16–22)				
Raman	IR	Raman	IR	Raman	IR	Raman	IR	assignm.[c,d]
3337–3340[e] w	3336–3344[e] s	3337–3340[e] w	3338–3342[e] s	3339–3340[e] w	3341–3343[e] s			amide A
	(3313)[f]		(3339)[f]		(3341)[f]			
	3088–3089[e] m		3090–3100[e] m		3087–3090[e] m			amide B
1733–1734 m	1734–1736 vs	1733–1734 m	1734–1736 vs	1730–1735 m	1735 vs	1732 m	1732 vs	ν[C=O(COOH)]
1643–1647 m		1648–1651 m		1646–1649 m		1647 s		amide I
1604–1605 vw	1608–1610 vs	1606–1609 vw	1606–1610 vs	1605–1608 vw	1607–1609 vs	1603 vw	1601 vs	
1559–1563 w		1557–1561 vw		1558–1562 w		1560 w		amide II
1539–1543 sh	1547–1551 s	1540–1547 sh	1543–1552 s	1537–1542 sh	1543–1547 s	1540 sh	1554 s	
1443–1444 m	1443–1444 w	1444–1446 m	1443 w	1443–1447 m	1443 w	1443 m	1441 w	
1417–1419 s	1414–1416 m	1416 s	1413–1415 m	1413–1418 s	1415–1416 m	1412 s	1417 m	s(CH_2)
	1408–1410 m		1408–1411 m		1408–1409 m		1408 m	
1342–1344 sh	1338–1340 vw	1345–1346 vw	1343–1348 vw	1342–1345 w		1340 sh		t(CH_2) + w(CH_2)
1322–1323 m		1321–1324 m		1318–1323 m		1318 m		
1297 m	1294 w	1298 m	1294–1295 w	1294–1300 m	1294–1295 w	1295 m	1295 w	amide III
1278–1280 m	1269–1275 m	1279–1281 m	1274–1275 m	1278–1283 m	1276–1277 m	1280 m	1280 m	
1234–1237 s	1215–1236 w	1233–1234 s	1237–1238 w	1231–1236 s	1237–1238 w	1230 s	1236 w	
1198–1201 w	1192–1194 w	1197–1200 w	1191–1192 m	1196–1200 w	1190–1191 m	1200 w	1190 m	w(CH_2)
1172–1173 w	1171–1173 s	1175–1176 w	1168–1170 s	1171–1174 w	1169–1170 s	1172 w	1168 s	
1116–1118 w	1120–1126 w	1115–1120 w	1119–1121 w	1115–1119 w	1118–1125 w	1116 w		
						1070 sh		
1063–1064 vs	1063–1065 vw	1062–1064 vs	1064 vw	1060–1064 vs	1064 vw	1059 vs	1035 vw	ν(C—N, C—O)
1015–1021 m	1016–1018 vw	1020–1021 m	1018 vw	1019–1023 m	1019–1020 vw	1021 m		
960–962 m		961–963 m		962–964 m		965 m		
943–947 vw	947–951 vw	935–940 vw	950–952 vw	935–942 vw	951–952 vw	941 vw	952 vw	ν(C—C)
899–902 w		903 w		900–902 m		900 w		
867–868 w	877–891 vw	869–870 vw	889–890 vw		888–889 vw	889 vw	885 vw	
825–832 vw	816–823 w	821–825 vw	816–818	823–827 vw	827–829 vw	826 w	834 vw	r(CH_2)
772–784 vw	793 m	773–775 vw	791–792 m	777–795 vw	791–792 m	772 vw	789 m	
662–676 vw		694–696 vw		691–693 vw		686 vw		amide V
633–639 vw	633–644 m	647–651 vw	635–641 m	640–648 vw	640–643 m	645 vw	638 m	amide IV
561–565 vw		566–568 vw		560–564 vw		562 vw		amide VI
488–497 vw	492–495 vw	493–495 vw	493–495 vw	490 vw	494–497 vw	497 vw	500 vw	δ[C=O(out)]
	480–483 w	487–489 vw	483 w	483–484 vw	483–484 w	484 vw	484 w	δ[C=O(in)]
	443–448 vw	462–464 vw	442 vw	443–459 vw	446 vw	458 vw	450 vw	
325–328 vw	317–321 vw	327–334 vw	320–321 vw	315 vw	319–320 w	330 vw	318 w	
304–311 vw		305–307 vw		298–302 vw		300 vw		backbone
274–276 vw		276–279 vw				280 vw		deformation
239–245 w	232–239 w		238–239 w		238–240 w		240 w	
	167–170 vw		170 vw		170–171 vw			

[a] Abbreviations as in Table 2. [b] Only the main vibrational bands characteristic of β_2-type are listed. For the shorter A-series oligomers (N = 3–6), the Raman and IR spectra are actually identical with those for the shorter B-series (N = 3–6). Therefore, the observed frequencies of the shorter B-series in Table 3 also contain those of the A-series samples. [c] From ref. 21 and 29. [d] Abbreviations for assignments as in Table 2. [e] Observed frequency. [f] Corrected for Fermi resonance.

medium length oligomers were measured in the solid state at monthly intervals, the β_2 characteristic bands at 238–239, 317–321, 444, 480–483 and 493–495 cm^{-1} began to appear and increase in intensity, until finally the accompanying β_1 characteristic bands became very weak shoulders.

The stability of the two β-forms of the oct-oligomers in the solid state and the dependence of residue number and conformational preference upon the specific method of crystallization of the sample were investigated by Raman and IR spectroscopy. The resulting conclusions support those derived from the X-ray diffraction powder patterns.

The amide A modes (NH stretching) are perturbed by the Fermi resonance between the amide A and amide B (the overtone modes of amide II). The unperturbed frequencies of the amide A modes are expected at 3297–3309 cm^{-1} for the β_1-type oligomers and at 3313–3341 cm^{-1} for the β_2-type oligomers.[32] These unperturbed frequencies are listed in Tables 2 and 3 with the observed frequencies. Even if anharmonicity effects are allowed, the unperturbed frequency of amide A for the β_1-type oct-oligomers is much lower than that for the β_2-type oligomers, indicating that the hydrogen bond in the β_1 type is considerably stronger than that in the β_2 type.

α-Helical Oligomers

The FTIR spectra for the transparent films of the oligomer series (N = 3–14), which were made by casting them from a DMF solution onto an NaCl plate or a KBr disc, were measured at room temperature and compared with those of the two β-forms[21] and the α-helical structure of poly(Glu).[29,31]

Fig. 4 shows the FTIR spectra of the cast films for the medium length oligomers (N = 8–14). These IR spectra cannot be interpreted by allocating the features to the β_1- or β_2-type structures,[21] but can be satisfactorily explained in terms of the α-helical structure.[32] The IR bands characteristic of the α-helix even appear in the cast films of the short oligomers (N = 3–6), as listed in Table 4.

The Fermi-resonance-perturbed frequencies and the unperturbed frequencies of the amide A modes for the α-helical oct-oligomers are also listed in Table 4. The unperturbed frequencies at 3267–3276 cm^{-1} for these α-helical oligomers are very close to the values of 3268 cm^{-1} for α-helical

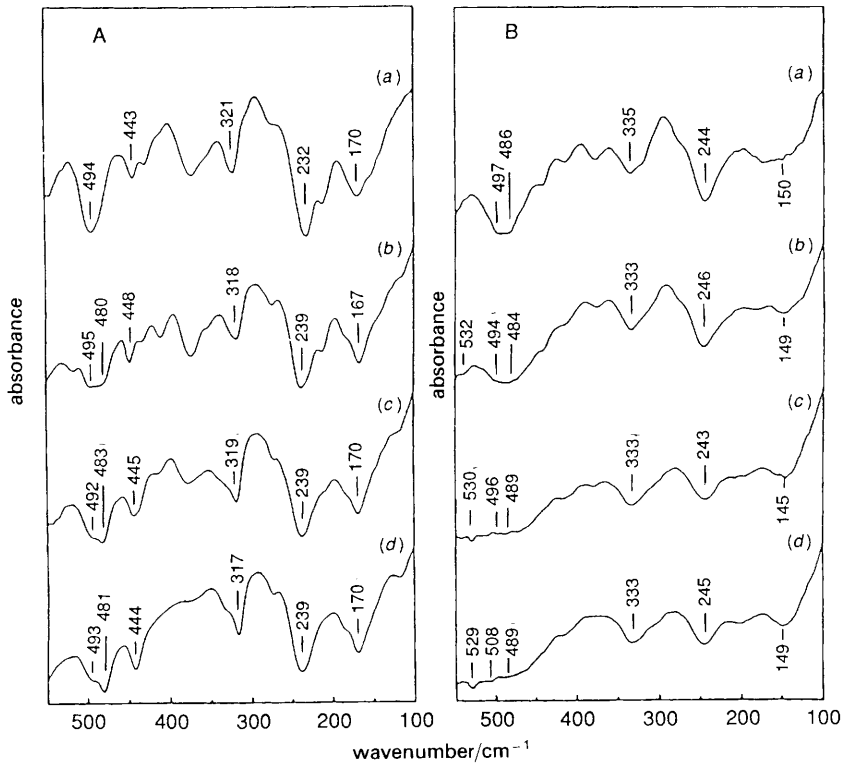

Fig. 3 FTIR spectra of oct-oligomers in the low-frequency region: A, (A-series samples, N = 3–6, β_2-type), N = 3 (*a*), 4 (*b*), 5 (*c*), 6 (*d*); B, (A-series samples, N = 8–22, β_1-type), N = 8 (*a*), 14 (*b*), 18 (*c*), 22 (*d*)

poly(Glu)[32] and 3279 cm^{-1} for α-$(Ala)_n$,[53] indicating a similarity between these oligomers and the polymers in the hydrogen-bonding environment. Moreover, the unperturbed frequencies found for the α-oct-oligomers imply that the hydrogen bond in the oligomers is stronger than that in the two β-forms of the oct-oligomers.

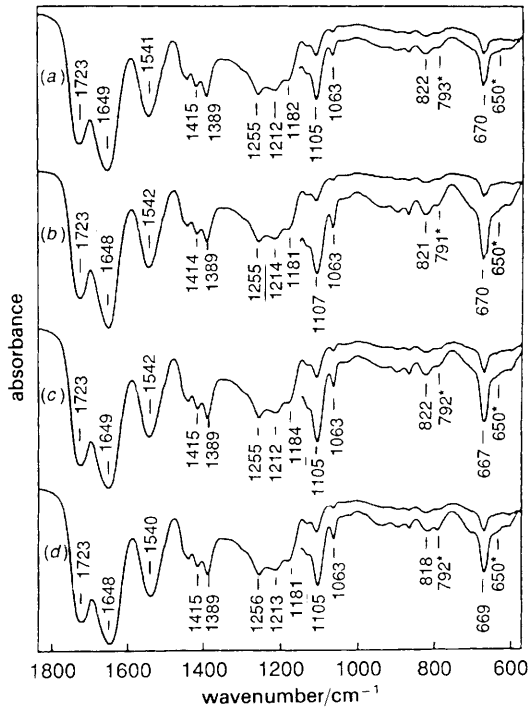

Fig. 4 FTIR spectra of the α-helical oct-oligomers: N = 8 (*a*), 10 (*b*), 12 (*c*), 14 (*d*) made by casting a DMF–oligomer solution onto an NaCl plate. The bands marked with an asterisk at 650 and 791–793 cm^{-1} may be due to disordered and β_2 conformations, respectively

The IR bands at 667–671 cm^{-1} are observed for all the cast films and closely correspond to the 670 cm^{-1} band of the α-helical structure of poly(Glu), which has been assigned to the amide V mode.[32] This observation provides ample evidence for the preferential stabilization of the α-helical structure in the cast films of the oligomers.

For the IR spectra of the oct-oligomers in Fig. 4, the very weak 791–793 cm^{-1} bands (marked with an asterisk) may arise from the small amounts of the unconverted β_2-type oligomers. Furthermore, the weak and broad bands at *ca.* 650 cm^{-1} (marked with an asterisk) may be due to the disordered conformation.[52] However, since the intensities of these IR bands are very weak, the populations of the β_2-type and disordered conformations may be very small.

For the oct-oligomers of residue number N = 3–14, the FTIR spectra of films cast onto a quartz disc were not characteristic of the α-helix, and their β_1 and β_2 characteristics remained unchanged. Therefore, the appearance of an α-helical structure for the oct-oligomers seems to be due to the material of the discs used as windows for the IR measurements, *i.e.*, NaCl or KBr salts on the surface of the windows may induce formation of the α-helix.

It has already been reported that the critical chain lengths for α-helix formation of homo-oligopeptides vary from 6 to 15 residues depending on the experimental conditions.[14,16,54–58] In the present study, the critical chain length (N = 3) for α-helix formation of the oct-oligomers is restricted by the surface of the salt plates. Therefore, this critical size is regarded as that induced by the salts.

The transparent films of the α-helical oligomers (N = 3–14) on the NaCl plate became turbid with time and these turbid films had properties of the β_2-type IR spectra. This observation reveals that the $\alpha \rightarrow \beta_2$ transition for the cast films occurs on the NaCl plate and that the α-helical structure is less stable than the β_2-type structure in the oligomer films. Instability of the α-helical structure was also observed in the case of poly(Glu).[21]

Table 4 Observed IR band frequencies (cm^{-1})[a] of α-helical oct-oligomers in cast films[b]

α-helical oct-oligomers (N)[c]							α-helical poly(Glu)[d]	assignm.[d]
3	4	6	8	10	12	14		
3292[e] s (3276)[f]	3290[e] s (3274)[f]	3282[e] vs (3274)[f]	3292[e] vs (3276)[f]	3292[e] vs (3274)[f]	3289[e] vs (3267)[f]	3284[e] vs (3272)[f]	3301[e] vs (3268)[f]	amide A
3072[e] s	3066[e] s	3074[e] s	3066[e] s	3066[e] s	3062[e] s	3068[e] s	3067[e]	amide B
1719 s	1719 s	1712 s	1723 s	1723 s	1723 s	1723 s	1718 s	ν[C=O(COOH)]
1646 vs	1642 vs	1644 vs	1649 vs	1648 vs	1649 vs	1648 vs	1653 vs	amide I
1544 s	1541 s	1541 s	1541 s	1542 s	1542 s	1540 s	1550 s	amide II
1450 sh	1449 sh	1449 sh	1449 sh	1450 sh	1449 sh	1449 sh	1451 w	s(CH_2)
1415 m	1415 m	1415 m	1415 m	1414 m	1415 m	1415 m	1417 m	
1389 m	1388 m	1388 m	1389 m	1389 m	1389 m	1389 m	1388 m	w(CH_2)
1342 vw	1338 vw	1340 sh	1339 vw	1342 vw	1339 vw	1338 vw	1343 sh	t(CH_2)
1295 sh	1295 sh	1294 sh	1291 sh	1289 sh	1289 sh	1290 sh	1283 w	amide III
1255 m	1254 m	1256 m	1255 m	1255 m	1255 m	1256 m	1253 ms	ν[C—O(COOH)]
1212 m	1212 m	1214 m	1212 m	1214 m	1212 m	1213 m	1212 m	w(CH_2)
1181 m	1183 m	1177 m	1182 m	1181 m	1184 m	1181 m	1181 w	H^{α} bend + t(CH_2)
1130 w	1130 w	1136 w	1128 w	1130 w	1128 w	1127 w	1118 w	ν(N—C^{α}), ν(C^{α}—C^{β})
1106 w	1106 w	1105 w	1105 w	1105 w	1105 w	1105 w	1083 w	ν(C^{α}—C^{β})
1063 vw	1063 vw	1063 vw	1063 vw	1063 vw	1063 vw	1063 vw	1060 w	
934 vw	934 vw	938 w	934 vw	935 vw	934 vw	938 vw	928 w, b	ν(C—N), ν(C^{α}—C)
897 vw	893 vw	899 vw	894 vw	894 vw	898 vw	893 vw	896 w	ν(C^{γ}—COOH)
866 vw	864 vw	865 vw	865 vw	865 vw	865 vw	865 vw	869 w	
818 vw	818 vw	810 vw	822 vw	821 vw	822 vw	818 vw	824 mw	γ(CH_2)
705 sh	705 sh	703 vw	705 vw	705 vw	706 vw	701 vw	705 w	CO_2 deformation
670 w	671 w	669 w	670 w	670 w	667 w	669 w	670 mw	amide V

[a] Abbreviations as in Table 2. [b] Only the main vibrational bands characteristic of the α-helix are listed. [c] N is the residue number of oct-oligomer. [d] From ref. 32. [e] Observed frequency. [f] Corrected for Fermi resonance.[32]

For the longer A-series oligomers ($N = 16$–22), transparent films were also cast from the DMF solution onto an NaCl plate, and their FTIR spectra investigated. These cast films showed superimposition of the IR spectra characteristic of both the β_1-type and the α-helix immediately after preparation of the film, showing coexistence of both these conformers. However, the IR bands characteristic of the α-helix decreased in intensity with time until they finally became weak shoulders, while the β_1-type IR bands became predominant. Thus, although the longer oligomers also take up the α-helical conformation, this structure is unstable on the NaCl plate and the β_1-type structure is preferentially stabilized with time.

Thus, the $\alpha \rightarrow \beta_2$ transition occurs for the cast films of the short and medium length oligomers while the $\alpha \rightarrow \beta_1$ transition is preferred by the long oligomers. This fact reveals that the residue number is directly correlated to the conformational preferences of the oct-oligomers on the salt plates.

Conclusions

From the X-ray diffraction powder patterns we may conclude that oct-oligomers take up β_1- or β_2-type conformations, similar to the two β-forms of poly(Glu),[21] depending upon the residue number.

The medium length A-series samples ($N = 8$–22) provide β_1-type powder patterns while the B-series samples with the same residue number ($N = 8$–22) yield β_2-type powder patterns. However, the shorter oligomers ($N = 3$–6) of both the A- and B-series provide only β_2-type powder patterns. These results imply that the specific method of crystallization of the sample is related to the conformational preference and that this also depends upon the residue number. Furthermore, the medium length oligomers ($N = 8$–14) of the A-series, which were kept at −20 °C for six months, provide β_2-type powder patterns at room temperature, indicating that a $\beta_1 \rightarrow \beta_2$ transition occurs and that the β_2-type structure is preferentially stabilized in the solid state.

The vibrational spectra provide ample evidence that the oct-oligomers take up both β_1- and β_2-type conformations, and that the oligomer films made by the casting method onto NaCl or KBr discs take up an α-helical structure. The IR spectra also reveal that the $\alpha \rightarrow \beta_2$ transition occurs for the short and medium length oligomers while the $\alpha \rightarrow \beta_1$ transition occurs for the long oligomers ($N = 16$–22).

The stability of the two β-forms and of the α-helical structure in the oct-oligomers seems to be dependent upon the residue number. For a more detailed discussion of their stability a kinetic study of the transitions is desirable. A study of the octyl chain effect on the α- and two β-forms in the oct-oligomers may also be required, since the long acyl chain must affect the conformations of the oligomer parts, as has been found for *N*-acylglycine oligomers.[11]

We express gratitude to Prof. Charmian J. O'Connor, Department of Chemistry, The University of Auckland, New Zealand for reading the manuscript prior to publication and making suggestions for its revision.

References

1 H. Michel and D. Oesterhelt, *Proc. Natl. Acad. Sci. USA*, 1980, **77**, 1283.
2 M. Garavito and J. P. Rosenbusch, *J. Cell Biol.*, 1980, **86**, 327.
3 H. Michel, *J. Mol. Biol.*, 1982, **158**, 567.
4 H. Michel, *Trends Biochem. Sci.*, 1983, **8**, 56.
5 R. M. Garavito, Z. Markovic-Housely and J-A. Jenkins, *J. Crystal Growth*, 1986, **76**, 701.
6 M. Roth, A. Lewit-Bentley, H. Michel, J. Deisenhofer, R. Huber and D. Oesterhelt, *Nature (London)*, 1989, **340**, 659.
7 H. Okabayashi, M. Okuyama and T. Kitagawa, *Bull. Chem. Soc. Jpn.*, 1975, **48**, 2264.
8 H. Okabayashi and M. Abe, *J. Phys. Chem.*, 1980, **84**, 999.
9 K. Tsukamoto, K. Ohshima, K. Taga, H. Okabayashi and H. Matsuura, *J. Chem. Soc., Faraday Trans. 1*, 1987, **83**, 789.
10 H. Okabayashi, K. Tsukamoto, K. Ohshima, K. Taga and E. Nishio, *J. Chem. Soc., Faraday Trans. 1*, 1988, **84**, 1639.
11 H. Okabayashi, K. Ohshima, H. Etori, R. Debnath, K. Taga and T. Yoshida, *J. Chem. Soc., Faraday Trans.*, 1990, **86**, 1561.
12 H. Okabayashi, K. Taga, T. Yoshida, K. Ohshima, H. Etori, T. Uehara and E. Nishio, *Appl. Spectrosc.*, 1991, **45**, 626.

13 M. Rinaudo and A. Domard, *Biopolymers*, 1975, **14**, 2035.
14 M. Goodman, A. S. Verdini, C. Toniolo, W. D. Philips and F. A. Bovey, *Proc. Natl. Acad. Sci. USA*, 1969, **64**, 444.
15 M. Goodman, F. Naider and C. Toniolo, *Biopolymers*, 1971, **1**, 1719.
16 A. Yaron, E. Katchalski, A. Berger, G. D. Fasman and H. A. Sober, *Biopolymers*, 1971, **10**, 1107.
17 G. M. Bonora and C. Toniolo, *Biopolymers*, 1974, **13**, 2179.
18 M. Rinaudo and A. Domard, *J. Am. Chem. Soc.*, 1976, **98**, 6360.
19 M. Rinaudo and A. Domard, *Macromolecules*, 1977, **10**, 720.
20 M. Mutter, *Macromolecules*, 1977, **10**, 1413.
21 K. Itoh, B. M. Foxman and G. D. Fasman, *Biopolymers*, 1976, **15**, 419.
22 M. L. Tiffany and S. Krimm, *Biopolymers*, 1968, **6**, 1379.
23 S. S. Zimmerman and L. Mandelkern, *Biopolymers*, 1975, **14**, 567.
24 E. M. Ambrose, *J. Chem. Soc.*, 1950, 3239.
25 E. R. Blout and M. Idelson, *J. Am. Chem. Soc.*, 1956, **78**, 497.
26 H. Lenormant, A. Baudras and E. R. Blout, *J. Am. Chem. Soc.*, 1958, **80**, 6191.
27 J. L. Koenig and B. Frushour, *Biopolymers*, 1972, **11**, 1871.
28 T. Miyazawa and E. R. Blout, *J. Am. Chem. Soc.*, 1961, **83**, 712.
29 G. D. Fasman, K. Itoh, C. S. Liu and R. C. Lord, *Biopolymers*, 1978, **17**, 1729.
30 P. Doty, A. Wada, J. T. Yang and E. R. Blout, *J. Polym. Sci.*, 1957, **23**, 851.
31 P. K. Sengupta and S. Krimm, *Biopolymers*, 1984, **23**, 1565.
32 P. K. Sengupta and S. Krimm, *Biopolymers*, 1985, **24**, 1479.
33 H. D. Keith, G. Giannoni and F. J. Padden, *Biopolymers*, 1969, **7**, 775.
34 H. D. Keith, F. J. Jr. Padden and G. Giannoni, *J. Mol. Biol.*, 1969, **43**, 423.
35 S. S. Zimmerman, J. C. Clark and L. Mandelkern, *Biopolymers*, 1975, **14**, 585.
36 Y. Mitsui, *Biopolymers*, 1973, **12**, 1781.
37 K. Rosenheck and P. Doty, *Biopolymers*, 1961, **47**, 1775.
38 S. Takashima, *Biopolymers*, 1963, **1**, 171.
39 G. Muller, F. Van del Touw, S. Zwolle and M. Mandel, *Biophys. Chem.*, 1974, **2**, 242.
40 H. Nakamura and A. Wada, *Biopolymers*, 1981, **20**, 2567.
41 S. Mashimo, T. Ota, N. Shinyashiki, S. Tanaka and S. Yagihara, *Macromolecules*, 1989, **22**, 1285.
42 A. R. Bizzarri, C. Cametti and F. Bordi, *J. Phys. Chem.*, 1990, **94**, 2166.
43 S. Nilsson and W. Zhang, *Macromolecules*, 1990, **23**, 5234.
44 L. Pauling and R. B. Corey, *Proc. Natl. Acad. Sci. USA*, 1951, **37**, 729.
45 E. J. Ambrose and A. Elliott, *Proc. R. Soc. London, A*, 1951, **205**, 47.
46 T. Miyazawa and E. R. Blout, *J. Am. Chem. Soc.*, 1961, **83**, 712.
47 K. Itoh and T. Shimanouchi, *Biopolymers*, 1970, **9**, 383.
48 A. Hashimoto, H. Aoyagi and N. Izumiya, *Bull. Chem. Soc. Jpn.*, 1980, **53**, 2926.
49 T. Uehara, H. Kojima, K. Taga, H. Okabayashi and T. Yoshida, *Chem. Exp.*, 1991, **6**, 639.
50 T. Miyazawa, T. Shimanouchi and S. Mizushima, *J. Chem. Phys.*, 1956, **24**, 408.
51 T. Miyazawa, T. Shimanouchi and S. Mizushima, *J. Chem. Phys.*, 1958, **29**, 611.
52 T. Miyazawa, Y. Masuda and K. Fukushima, *J. Polym. Sci.*, 1962, **62**, S62.
53 S. Krimm and A. M. Dwivedi, *J. Raman Spectrosc.*, 1982, **12**, 133.
54 C. Toniolo, G. M. Bonora and M. Mutter, *Int. J. Biol. Macromol.*, 1979, **1**, 188.
55 C. Toniolo, G. M. Bonora, S. Salardi and M. Mutter, *Macromolecules*, 1979, **12**, 620.
56 G. M. Bonora, C. Toniolo and M. Mutter, *Polymer*, 1978, **19**, 1382.
57 C. Toniolo, G. M. Bonora, M. Mutter and V. N. R. Pillai, *Makromol. Chem.*, 1981, **182**, 1997.
58 C. Toniolo, G. M. Bonora, H. Anzinger and M. Mutter, *Macromolecules*, 1983, **16**, 147.

Paper 2/02704F; *Received* 26*th May*, 1992